POLYVINYL ALCOHOL NANOFIBROUS MEMBRANE BY HIGH-CURVATURE SOLID-NEEDLE ELECTROSPINNING
Numerical Simulation and Experimental Verification

by

Zhen-Zhen XU[a], Qin-Qin YANG[a], Bing GAO[a], Kai-Zhun LI[a], Ming-Qiang GUAN[c], Jiang-Hui ZHAO[a*], and Zhi LIU[a,b,c*]

[a] School of Textile and Garment, Anhui Polytechnic University, Wuhu, China
[b] CETC Wuhu Diamond Aircraft Manufacture CO., Ltd., Wuhu, China
[c] Anhui Hebang Textile Technology CO., Ltd., Bozhou, China

Original scientific paper
https://doi.org/10.2298/TSCI2303993X

Herein, polyvinyl alcohol nanofibrous membrane was fabricated firstly by the high-curvature solid-needle electrospinning. The influence of electrode curvature (needle angle), spinning voltage, solution concentration and collector distance on nanofiber morphology was systematically investigated numerically and experimentally. Numerical simulation shows that the electrical field increases with the increase of spinning voltage, while decreases with the increase of needle angle and collector distance. The experimental results are consistent with the numerical results. Furthermore, the solution concentration can be used to adjust the diameter of polyvinyl alcohol nanofibers. The possible applications of the nanofiber membrane to energy generation, water treatment, and separation are also discussed.

Key words: *high curvature, solid needle, polyvinyl alcohol, numerical simulation, separation*

Introduction

Nanofiber membranes can now be easily fabricated by either the bubble electrospinning [1-4] or the traditional electrospinning [5-7]. Nanofibers, especially, carbon nanotubes, possess superior properties and are applied in various areas including composites [8], nanofluids [9], energy harvesting [10], and separation and filtration [11, 12], and nanofiber membranes with hierarchical structure always have attractive properties [13]. Polyvinyl alcohol (PVA) shows many excellent characteristics such as good biocompatibility, mechanical property, fiber formability, chemical resistance, moisture affinity, making it an ideal materials for biomedicine applications [14]. Jatoi *et al.* [15] synthesized carbon nanotube-silver nanoparticle-PVA nanofiber membrane for wound healing applications. Azarian *et al.* [16] fabricated chloroacetated natural rubber-PVA nanofiber membrane encapsulated with kaolin and starch for wood dressing. Wei *et al.* [17] reported cross-linked PVA-silver nanoparticle nanofiber membrane with antibacterial property. Similarly, Sekar *et al.* [18] reported Fe-doped ZnO nanoparticles/PVA nanofiber for antibacterial application.

Due to its moisture affinity, PVA nanofibers disappear in water. Therefore, PVA nanofiber membrane can be cross-linked to apply in water treatment such as removal of heavy

* Coresponding authors, e-mail: zhaojh@ahpu.edu.cn, liuzhi@ahpu.edu.cn

mental ions. Ullah *et al.* [19] crosslinked PVA nanofiber by glutaraldehyde vapors to remove heavy mental ions. Tian *et al.* [20] fabricated crosslinked PVA nanofiber membrane for heavy mental remove. The resulting membrane can achieve the adsorption equilibrium time of Pb^{2+} decrease from 30 to 10 hours and Cu^{2+} decrease from 15 to 5 hours, respectively.

In the application in terms of wound healing and heavy mental remove, the PVA diameter and diameter distribution is very important. The high-curvature solid-needle electrospinning can fabricate ultrafine nanofiber under low voltage supply. Therefore, the investigation of parameters influence on PVA nanofiber morphology by high-curvature solid-needle electrospinning is helpful for the PVA nanofiber preparation and application.

In the present study, we systematically investigated the parameters influence on nanofiber morphology. We aim to the effect of electrode curvature (needle angle), voltage supply, and collector distance on the PVA nanofiber morphology by numerical simulation and experimental verification, and the effect of solution concentration on the PVA nanofiber morphology. The results benefit the preparation and application of PVA nanofibrous membrane by high-curvature solid-needle electrospinning.

Experimental

Materials

The PVA (1750±50) was purchased from Sinopharm Chemical Reagent Co., Ltd. (Suzhou, China). The deionized water is made in the laboratory. Reagent was analytical grade and was used as received without further treatment.

Preparation of PVA nanofiber by high-curvature solid-needle electrospinning

The spinning solution was achieved by dissolving PVA into deionized water after stirring at 98 °C for 3 hours. To investigate the effect of needle angle on nanofiber morphology, the needle angle defined in [21], the needle angles of 30°, 60°, 90°, and 120° were used in the spinning, tab. 1. To investigate the effect of voltage supply on nanofiber morphology, the voltage chose as 8 kV, 11 kV, 15 kV, and 20 kV, tab. 1. To investigate the effect of collector distance on nanofiber morphology, the collector distance chose as 6 cm, 14 cm, and 22 cm, tab. 1. To investigate the effect of solution concentration on nanofiber morphology, the PVA solution concentration chose as 8 wt.%, 10 wt.%, 12 wt.%, 14 wt.%, and 16 wt.%, tab. 1.

Table 1. Spinning parameters of investigating the needle curvature influence

Variable	Needle angle [°]	Voltage [kV]	Collection distance [cm]	Concentration [%]
Needle angle	**30, 60, 90, 120**	11	14	8
Voltage	60	**8, 11, 15, 20**	14	8
Collection distance	60	11	**6, 14, 22**	8
Concentration	60	11	14	**8, 10, 12, 14, 16**

Characterization

The morphology of the regenerated electrospun nanofibers were observed by SEM (Hitachi S-4800, Japan). The diameters of nanofibers were calculated by measuring at least 100 fibers at random using IMAGE *J* program. The electric field around the solid needle was calculated by using Maxwell 2D (ANSOFT Corporation). The Maxwell program utilizes finite element methods and adaptive meshing to achieve a converged solution. In the simulation process, the calculation finished at energy error of 0.045% and delta energy of 0.43% [21, 22].

Results and discussion

The effect of needle angle on PVA nanofiber morphology

The schematic diagram of PVA nanofiber by high-curvature solid-needle electrospinning was shown in fig. 1. The apparatus was similar to traditional single needle electrospinning except for the spinning electrode, figs. 1(a) and 1(b). The practical spinning process is presented in fig. 1(c), indicating stable spinning process. The electrode shape is the key factor affecting the electrical field and the subsequent nanofiber morphology [23, 24]. As shown in figs. 2(e)-2(h), with the increase of needle angle (decrease of needle curvature), the electrical field around the needle tip decreases. The nanofiber diameter change is in accordance with the numerical simulation results that the nanofiber diameter increases with the the increase of needle angle, figs. 2(a)-2(d). At the needle angle of 30°, the high curvature induces strong electrical field up to $1.88 \cdot 10^5$ V/m, resulting in smaller nanofiber diameter of 224.1 ±39.4 nm, figs. 2(a) and 2(e), tab. 2. At the needle angle of 60°, the electrical field is $1.56 \cdot 10^5$ V/m and the resulting nanofiber diameter is 244.0 ±41.5 nm, figs. 2(b) and 2(f), tab. 2. At the needle angle of 90°, the electrical field and nanofiber diameter are $1.50 \cdot 10^5$ V/m and 257.0 ±36.2 nm, respectively, figs. 2(c) and 2(g), tab. 2. While the electrical field decreases to $1.31 \cdot 10^5$ V/m at the needle angle of 120°, the weakened electrical field leads to increased nanofiber diameter of 267.8 ±34.4 nm, figs. 2(d) and 2(h), tab. 2.

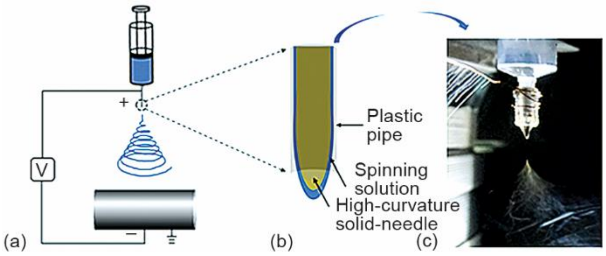

Figure 1. The schematic diagram of PVA nanofiber by high-curvature solid-needle electrospinning; (a) the schematic diagram of high-curvature solid-needle electrospinning, (b) the schematic diagram of high-curvature solid-needle, and (c) the optical image of practical spinning process of high-curvature solid-needle electrospinning

The effect of voltage supply on nanofiber morphology

The voltage has significantly effect on the spinning process and the resulting nanofiber morphology [25]. As displayed in fig. 3, with the increase of voltage supply, the diameter of resulting nanofiber decreases. The numerical simulation results further prove the experimental results, that is, the electrical field is increase with the voltage increase. The enhanced electrical field leads to the decrease of nanofiber diameter. At the voltage of 8 kV, the electrical field is $1.14 \cdot 10^5$ V/m and the resulting nanofiber diameter is 307.4 ±69.5 nm, figs. 3(a) and 3(e), tab. 2. At the voltage of 11 kV, the electrical field and the resulting nanofiber diameter are $1.56 \cdot 10^5$ V/m, 244.0 ±41.5 nm, respectively, figs. 3(b) and 3(f), tab. 2. At the voltage of 15 kV, the electrical field around the needle tip and the resulting nanofiber diameter are $2.13 \cdot 10^5$ V/m, 232.9 ±29.1 nm, respectively, figs. 3(c) and 3(g), tab. 2. At the voltage of 20 kV, the electrical field around the needle tip increases to $2.84 \cdot 10^5$ V/m, resulting in the smallest nanofiber diameter of 178.3 ±18.9 nm, figs. 3(d) and 3(h), tab. 2.

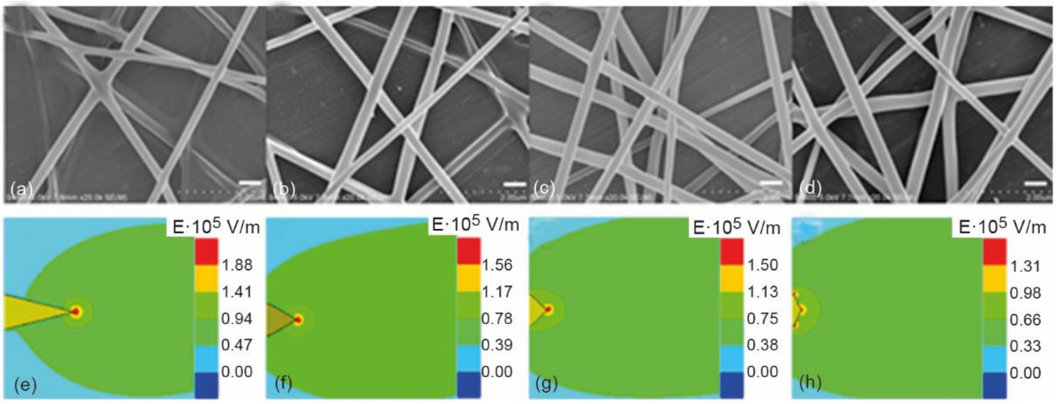

Figure 2. The resulting nanofiber morphology and electrical field around the needle tip at different needle angles; (a), (e) – 30°, (b), (f) – 60°, (c), (g) – 90°, (d), (h) – 120° (the scale bar is 500 nm)

Table 2. Nanofiber diameter under different spinning parameters

Needle curvature [°]	Diameter [nm]	Voltage [kV]	Diameter [nm]	Collection distance [cm]	Diameter [nm]	Concentra-tion [%]	Diameter [nm]
30	224.1 ±39.4	8	307.4 ±69.5	6	200.9 ±37.7	8	153.6 ±53.4
60	244.0 ±41.5	11	244.0 ±41.5	14	244.0 ±41.4	10	244.0 ±41.5
90	257.0 ±36.2	15	232.9 ±29.1	22	272.9 ±61.0	12	296.2 ±78.9
120	267.8 ±34.4	20	178.3 ±18.9	–	–	14	303.7 ±45.7
–	–	–	–	–	–	16	435.7 ±64.2

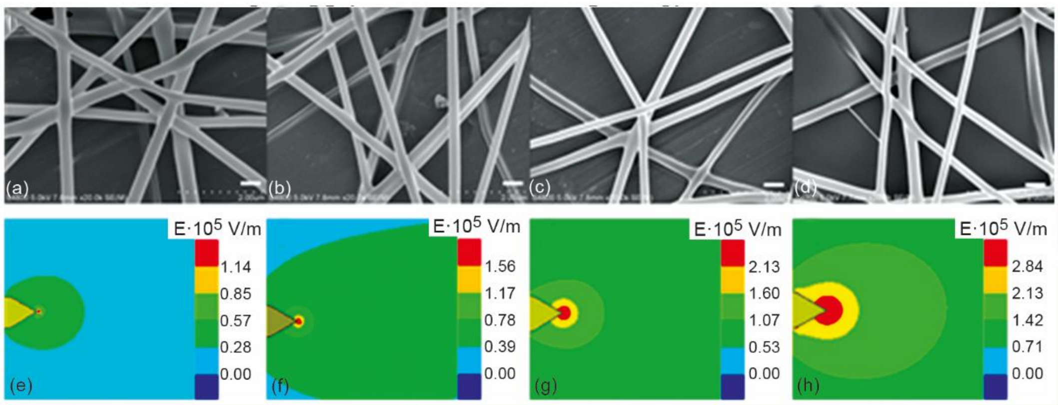

Figure 3. The resulting nanofiber morphology and the electrical field around the needle tip at different voltage supply; (a), (e) – 8 kV, (b), (f) – 11 kV, (c), (g) – 15 kV, and (d), (h) – 20 kV (the scale bar is 500 nm)

The effect of collector distance on nanofiber morphology

In the spinning process, the collector distance is also the key factor affecting the spinning process, nanofiber productivity and nanofiber morphology. Therefore, the collector distances of 6 cm, 14 cm, and 22 cm (voltage 11 kV and needle angle 60°) were chose to investigate the influence on the nanofiber morphology. As shown in the fig. 4(d), the collector distance of 6 cm induces the strongest electrical field up to $2.86 \cdot 10^5$ V/m, achieving the nanofiber diameter of 200.9 ±37.7 nm, tab. 2. However, the fibers stick to each other due to the no fully evaporated solvent under small collector distance, fig. 4(a). At the collector distance of 14 cm, the electrical field is $1.56 \cdot 10^5$ V/m, fig. 4(e), and the resulting nanofiber shows smooth morphology with fiber diameter of 244.0 ±41.4 nm, tab. 2. When the collector distance increases to 22 cm, the electrical field decreases to $1.20 \cdot 10^5$ V/m, fig. 4(f), obtaining the nanofiber diameter of 272.9 ±61.0 nm, tab. 2.

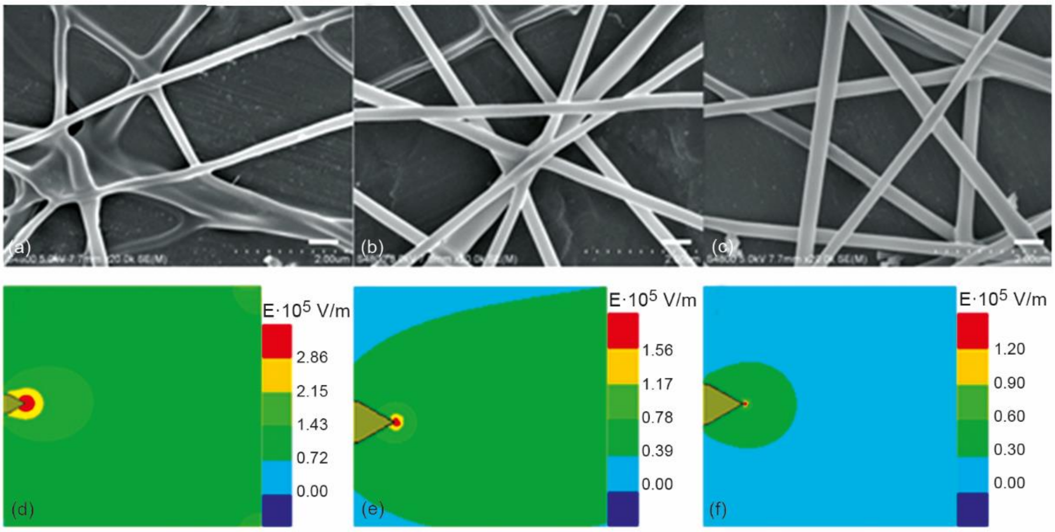

Figure 4. The resulting nanofiber morphology and the electrical field around the needle tip at different collector distances; (a), (d) – 6 cm, (b), (e) – 14 cm, and (c), (f) – 22 cm (the scale bar is 500 nm)

The effect of solution concentration on nanofiber morphology

Solution concentration crucially affects the nanofiber morphology. The nanofiber with different nanofiber diameter can be obtained by various solution concentration. As illustrated in fig. 5, the fibers partly stick to each other with fiber diameter 153.6 ±53.4 nm under the solution concentration of 8%, suggesting poor spinning ability at this situation, fig. 5(a). With the solution change from 10-16%, PVA nanofibers with smooth morphology are achieved and the resulting nanofiber diameter changes from 200.9 ±37.7 nm to 435.7 ±64.2 nm, indicating wide rages of fiber diameter towards different necessaries in practical application, figs. 5(b)-5(e) [26-28]. The results show that the diameter can be adjusted under different solution concentration by high-curvature solid-needle electrospinning.

Conclusions

The PVA nanofiber was successfully fabricated by high-curvature solid-needle electrospinning. Furthermore, the spinning parameters in terms of needle angle, voltage supply and collector distance were systematically studied both by numerical simulation and experimental verification. The results show that using needle angle 60°, voltage 11 kV and collector distance 14 cm can result in PVA nanofiber with smooth morphology and proper fiber diameter.

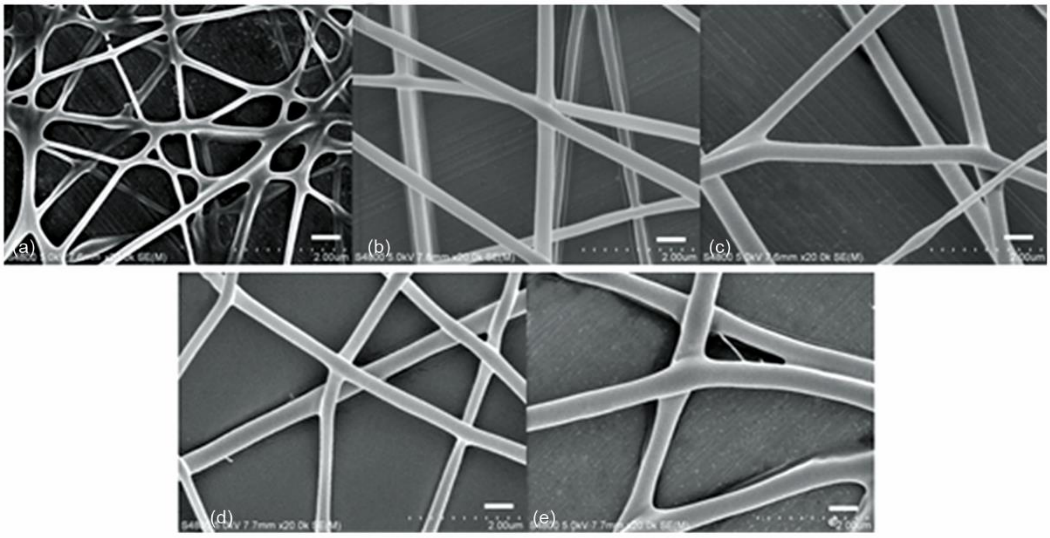

Figure 5. The resulting nanofiber morphology and the electrical field around the needle tip at different solution concentrations; (a) – 8%, (b) – 10%, (c) – 1%, (d) – 14%, and (e) – 16% (the scale bar is 500 nm)

Additionally, wide range fiber diameter can be achieved by regulating the solution concentration, suggesting adjustable membrane performance towards different applications. The results lay the foundation for the PVA preparation by high-curvature solid-needle electrospinning and applications regarding water treatment, energy generation and other related areas.

Acknowledgment

The authors would like to thank the support by National Natural Science Foundation of China (52003002), the Foundation Research of Anhui Polytechnic University (Xiky2022082), the Major Special Projects of Bozhou, Young and Middle-aged Top Talent Program by Anhui Polytechnic University.

References

[1] Li, X. X., He, J. H. Bubble Electrospinning with an Auxiliary Electrode and an Auxiliary Air Flow, *Recent Patents on Nanotechnology, 14* (2020), 1, pp. 42-45
[2] Liu, G. L., *et al*., Last Patents on Bubble Electrospinning, *Recent Patents on Nanotechnology, 14* (2020), 1, pp. 5-9
[3] Qian, M. Y., He, J. H., Collection of Polymer Bubble as a Nanoscale Membrane, *Surfaces and Interfaces, 28* (2022), Feb., 101665
[4] He, J. H., *et al*., The Maximal Wrinkle Angle During the Bubble Collapse and Its Application to the Bubble Electrospinning, *Frontiers in Materials, 8* (2022), 800567
[5] Liu, L. G., *et al*., Dropping in Electrospping Process: A General Strategy for Fabrication of Microspheres, *Thermal Science, 25* (2021), 2B, pp. 1295-1303
[6] Lin, L., *et al*., Fabrication of PVDF/PES Nanofibers with Unsmooth Fractal Surfaces by Electrospinning: A General Strategy and Formation Mechanism, *Thermal Science, 25* (2021), 2B, pp.1287-1294
[7] Tian, D., *et al*., Hierarchical Aligned ZnO Nanorods on Surface of PVDF/Fe2O3 Nanofibers by Electrospinning in a Magnetic Field, *Thermal Science, 25* (2021), 3B, pp. 2399-2403

[8] Wang, K. J., Wang, G. D., Study on the Nonlinear Vibration of Embedded Carbon Nanotube *via* the Hamiltonian-Based Method, *Journal of Low Frequency Noise, Vibration & Active Control*, *41* (2022), 1B, pp. 112-117
[9] Alous, S., *et al*., Experimental Study About Utilization of MWCNTs and Graphene Nanoplatelets Water-Based Nanofluids in Flat Non-Concentrating PVT Systems, *Thermal Science*, *25* (2021), 1B, pp. 477-489
[10] Feng Y., *et al*., Ultrahigh Discharge Efficiency and Excellent Energy Density in Oriented Core-Shell Nanofiber-Polyetherimide Composites, *Energy Storage Materials*, *25* (2020), Mar., pp. 180-192
[11] Liu Z., *et al*., Recent Progress of the Needleless Electrospinning for High Throughput of Nanofibers, *Recent Patents on Nanotechnology, 13* (2019), 3, pp. 164-170
[12] Choi, H. Y., *et al*., Thiol-Functionalized Cellulose Nanofiber Membranes for the Effective Adsorption of Heavy Metal Ions in Water, *Carbohydrate Polymers, 234* (2020), Apr., 115881
[13] Liu ,F., *et al*., Thermal Oscillation Arising in a Heat Shock of a Porous Hierarchy and Its Application, *Facta Universitatis Series: Mechanical Engineering*, *20* (2021), 3, pp. 633-645
[14] Liu, Z., *et al*., Polyvinyl Alcohol/Starch Composite Nanofibers by Bubble Electrospinning, *Thermal Science*, *18* (2014), 5, pp. 1473-1475
[15] Jatoi, A. W., *et al*., Antibacterial Efficacy of Poly (Vinyl Alcohol) Composite Nanofibers Embedded with Silver-Anchored Silica Nanoparticles, J*ournal of Biomedical Materials Research Part B: Applied Biomaterials*, *16* (2018), 3, pp. 1121-1128
[16] Azarian, M. H., *et al*., Biocompatibility and Biodegradability of Filler Encapsulated Chloroacetated Natural Rubber/Polyvinyl Alcohol Nanofiber for Wound Dressing, *Materials Science and Engineering: C, 103* (2019), Oct., 109829
[17] Wei, Y. S., *et al*., In Situ Synthesis of High Swell Ratio Polyacrylic Acid/Silver Nanocomposite Hydrogels and their Antimicrobial Properties, *Journal of Inorganic Biochemistry, 164* (2016), Nov., pp. 17-25
[18] Sekar, A. D., *et al*., Electrospinning of Fe-doped ZnO Nanoparticles Incorporated Polyvinyl Alcohol Nanofibers for Its Antibacterial Treatment and Cytotoxic Studies, *European Polymer Journal*, *118* (2019), Sept., pp. 27-35
[19] Ullah, S., *et al*., Stabilized Nanofibers of Polyvinyl Alcohol (PVA) Crosslinked by Unique Method for Efficient Removal of Heavy Metal Ions, *Journal of Water Process Engineering*, *33* (2020), Feb., 101111
[20] Tian, H., *et al*., Electrospinning of Polyvinyl Alcohol into Crosslinked Nanofibers: An Approach to Fabricate Functional Adsorbent for Heavy Metals, *Journal of Hazardous Materials, 378* (2019), Oct., 120751
[21] Liu, Z., *et al*., Needle-Disk Electrospinning: Mechanism Elucidation, Parameter Optimization and Productivity Improvement, *Recent Patents on Nanotechnology, 14* (2020), 1, pp. 46-55
[22] Liu, Z., *et al*., Electrospun Jets Number and Nanofiber Morphology Effected by Voltage Value: Numerical Simulation and Experimental Verification, *Nanoscale Research Letters, 14* (2019), 1, pp. 1-9
[23] Kang, D. H., *et al*., Advanced Electrospinning Using Circle Electrodes for Freestanding PVDF Nanofiber film Fabrication, *Applied Surface Science, 455* (2018), Oct., pp. 251-257
[24] Zhao, J., *et al*., Needle's Vibration in Needle-Disk Electrospinning Process: Theoretical Model and Experimental Verification, *Journal of Low Frequency Noise, Vibration and Active Control, 38* (2019), 3-4, pp. 1338-1344
[25] Zhou, H., *et al*., The Relationships Between Process Parameters and Polymeric Nanofibers Fabricated Using A Modified Coaxial Electrospinning, *Nanomaterials, 9* (2019), 6, 9060843
[26] Liu, Y. Q., *et al*., Nanoscale Multi-Phase Flow and Its Application To Control Nanofiber Diameter, *Thermal Science, 22* (2018), 1A, pp. 43-46
[27] Zhang, Y., *et al*., Optimizing the Dielectric Energy Storage Performance in P(VDF-HFP) Nanocomposite by Modulating the Diameter of PZT Nanofibers Prepared *via* Electrospinning, *Composites Science and Technology, 184* (2019), Nov., pp. 107838
[28] Wang, Q. L., *et al*., Intelligent Nanomaterials for Solar Energy Harvesting: From Polar Bear Hairs to Unsmooth Nanofiber Fabrication, *Frontiers in Bioengineering and Biotechnology, 10* (2022), July, 926253

Paper submitted: December 5, 2021
Paper revised: March 3, 2022
Paper accepted: March 10, 2022